IPNO-DRE 97-05

ISOMERIC M3 TRANSITIONS IN ^{183}Pt AND ^{181}Os

B. Roussière, P. Kilcher, A. Wojtasiewicz, J. Genevey, A. Gizon,
F. Ibrahim, A. Knipper, F. Le Blanc, G. Marguier, J. Obert,
J. Oms, J.C. Putaux, M. Ramdhane, J. Sauvage
and the ISOLDE collaboration

soumis à Nuclear Physics A

Isomeric M3 transitions in ^{183}Pt and ^{181}Os

B. Roussière [a], P. Kilcher [a], A. Wojtasiewicz [a,1], J. Genevey [b], A. Gizon [b], F. Ibrahim [a,2], A. Knipper [c], F. Le Blanc [a], G. Marguier [d], J. Obert [a], J. Oms [a], J.C. Putaux [a], M. Ramdhane [e], J. Sauvage [a] and the ISOLDE collaboration

[a] *Institut de Physique Nucléaire, CNRS-IN2P3/Université Paris 11, F-91406 Orsay Cedex, France*

[b] *Institut des Sciences Nucléaires, CNRS-IN2P3/Université Joseph Fourier, F-38026 Grenoble Cedex, France*

[c] *Centre de Recherches Nucléaires, CNRS-IN2P3/Université Louis Pasteur, F-67037 Strasbourg Cedex 2, France*

[d] *Institut de Physique Nucléaire, CNRS-IN2P3/Université Lyon I, F-69622 Villeurbanne Cedex, France*

[e] *PPE Division, CERN, CH-1211 Geneva 23, Switzerland*

The M3 transitions linking the isomeric and ground states in $^{183}_{78}Pt_{105}$ and $^{181}_{76}Os_{105}$ have been searched by high-resolution conversion-electron measurements. The reduced M3 transition probabilities have been estimated and compared to the values measured in neighbouring isotones ($^{179}_{74}W_{105}$ and $^{184}_{79}Au_{105}$). This comparaison confirms the particle configurations describing the ^{184}Au isomeric and ground states, $\pi h\frac{9}{2}\otimes\nu\frac{1}{2}[521]$ and $\pi h\frac{9}{2}\otimes\nu\frac{7}{2}[514]$, respectively. On the other hand, hindrance factors have been deduced. They show an unexpected sensitivity against Z.

Key words: Radioactivity ^{183,181}Hg. (β^+, EC) [from Pb(p, 3pxn)Hg, on-line mass separation], measured E_{e^-}, I(ce). γ-multipolarity. Reduced M3 transition probabilities. Magnetic spectrograph.

1 Introduction

The M3 transition in ^{184}Au, discovered by the NICOLE collaboration at ISOLDE [1] and then confirmed at ISOCELE [2], was quite unexpected in

[1] Permanent address : Warsaw University, Warsaw, Poland

[2] Present address : Institut des Sciences Nucléaires, F-38026 Grenoble, France

this odd-odd nucleus. Indeed, this M3 transition is the signature of an isomeric state, which was not detected in the first radioactivity study [3]. This has caused a revival of interest in this odd-odd nucleus located at the prolate border of the N $\sim$ 108, Z $<$ 82 shape transition region. Consequently experimental studies have been performed in order to determine the spins and parities of the ground and isomeric states of ^{184}Au [4], and to identify the proton-neutron shell-model configurations ($\pi \otimes \nu$) present in the low-energy spectrum of this nucleus [4,5]. The resulting assignments are $I^{\pi} = 2^{+}$ for ^{184m}Au and $I^{\pi} = 5^{+}$ for ^{184g}Au, together with proposing $\pi h\frac{9}{2} \otimes \nu\frac{1}{2}[521]$ and $\pi h\frac{9}{2} \otimes \nu\frac{7}{2}[514]$ configurations for these two states, respectively.

However, some aspects of this M3 isomeric transition remained puzzling, since the only case of an M3 transition linking the $\nu\frac{1}{2}[521]$ and $\nu\frac{7}{2}[514]$ states known so far was the one in ^{179}W, which occurs with an hindrance factor over the Weisskopf value at least thirty times higher than in ^{184}Au. Did we have to question the $\pi \otimes \nu$ configurations proposed in ref. [4] to describe the isomeric and ground states in ^{184}Au, or to put forward an abnormally high hindrance in ^{179}W ?

In order to get a deeper insight into the problem, we have undertaken a search for M3 isomeric transitions in ^{183}Pt and ^{181}Os, both isotones of ^{179}W and ^{184}Au, exhibiting the same $\nu\frac{7}{2}[514]$ and $\nu\frac{1}{2}[521]$ states as isomeric and ground states. No evidence for isomeric transitions was obtained in the previous studies of the ^{183}Pt and ^{181}Os low spin states [6,7], especially in ^{181}Os where the M3 transition had been searched [8] even before the energy of the isomeric state was known.

Besides this experimental work, we have studied the systematics of the M3 isomeric transitions taking as starting point the compilations available in this field [9–12]. In addition to update the existing experimental data, our study aimed to analyse the properties of the M3 transitions especially as a function of the particle configurations involved and to compare the M3 transitions in odd and odd-odd nuclei.

In this paper, we firstly present the search for the isomeric transitions in ^{183}Pt and ^{181}Os. In view of the low energy (E $<$ 50 keV) and the high multipolarity (M3) expected for these transitions, the best tool consists in carrying out low-energy internal-conversion-electron measurements with an energy resolution high enough to separate the L-lines and even the M-lines. Thus the multipolarity of the transitions can be unambiguously determined from the $L_1/L_2/L_3/\ldots$ intensity ratios. We then display the experimental results obtained in ^{183}Pt and ^{181}Os. Lastly, after having presented the systematics of the M3 transitions known in the literature, we discuss those observed in the four N = 105 isotones : ^{179}W, ^{181}Os, ^{183}Pt and ^{184}Au.

2 Experimental procedure

2.1 Experimental setup

States in ^{183}Pt and ^{181}Os are populated through the decay of ^{183}Hg and ^{181}Hg mass-separated sources. Mercury atoms are produced at ISOLDE (CERN) by bombarding a molten lead target [13] by the PS-Booster 1 GeV proton beam. The radioactive Hg ions extracted from the ion source are mass-separated and switched through a beam line onto the experimental setup devoted to the detection of low-energy conversion electrons with high energy resolution [14]. This apparatus consists of a semi-circular magnetic spectrograph associated with a tape transporter, a decelerating lens for the incoming ions and a preacceleration system for the electrons. Installed at first at the on-line isotope separator ISOCELE (acceleration high voltage = 44 kV), it has been modified to work on line with the ISOLDE separator (acceleration high voltage = 60 kV). Aluminium deposits 15 mm long and 9 mm wide have been evaporated each 7.5 cm onto the insulating tape used for the ion transport. The radioactive Hg ions are slowed down from 60 kV to 700 V before being collected on the Al deposits. In this way, the 59.3 kV high voltage, opposite to the acceleration high voltage, is applied only at the collection point. The deceleration of the ions before collection prevents them from being too deeply implanted and so preserves high energy-resolution measurements for the very low-energy electrons. The radioactive source is then moved into the spectrograph where a preacceleration high voltage is applied to accelerate the conversion electrons emitted by the source in order to overcome the energy cutoff due to the minimum radius of the spectrograph and then to allow the very low-energy electrons to reach the photographic film (Kodak, DEF392) used as a detector. The magnetic induction (B) and the preacceleration high voltage (HV) applied define the energy range of the conversion electrons detected : with B = 54×10^{-4} T and HV = -10 kV, a conversion-electron energy range 1-90 keV is covered.

2.2 Measurements achieved

Three measurements were carried out during the experiments. The first one was performed using ^{187}Hg mass-separated sources. Two exposures corresponding to different experimental conditions, i.e. without and with preacceleration high voltage, were achieved on the same photographic film. The following counting cycles ($t_{collection}$ = 480 s, $t_{waiting}$ = 120 s and $t_{measurement}$ = 600 s) were used to favour the ^{187}Au ($T_{\frac{1}{2}}$ = 8.4 m) decay among the radioactive chain issued from ^{187}Hg ($T_{\frac{1}{2}}$ = 2.4 m). As the energy and intensity of

the electron transitions belonging to the $^{187}Au \rightarrow {}^{187}Pt$ decay are well known [15], the obtained film has allowed us to determine precise values for both the magnetic induction and preacceleration high voltage as well as the response of the detection system (spectrograph+film) as a function of the impact energy of the electrons.
The second measurement was performed using ^{183}Hg ($T_{\frac{1}{2}} = 8.8$ s) mass-separated sources. The collection-measurement cycle was chosen to optimize the counting rate corresponding to the decay of ^{183m}Pt ($T_{\frac{1}{2}} = 43$ s) : the ^{183}Hg ions were collected during 160 s and the source activity counted for 160 s immediatly after each collection.
The third measurement was carried out with ^{181}Hg ($T_{\frac{1}{2}} = 3.6$ s) mass-separated sources using the following counting cycle : $t_{collection} = t_{measurement} = 900$ s, in order to favour the ^{181m}Os ($T_{\frac{1}{2}} = 2.7$ m) decay. No preacceleration was applied to the conversion electrons emitted since the main purpose of the experiment was the search for the isomeric M3 transition the energy of which, known from the location of the isomeric state in ^{181}Os (48.9 keV) [7], is not very low. In this case, the conversion-electron energy range covered was from 11 keV to 100 keV.

After development, the photographic films were analysed with a microdensitometer at the CDSI Institut d'Optique (Orsay). They have been scanned with a 400 μm height and 50 μm width slit : the blackening density was digitized and stored into a bidimensional x×y matrix where x represents, on the film, the position of the scanner in length and y in width. Electron spectra were then extracted from this matrix and analysed using programs working on the VAX 6000-510 computer at Orsay.

2.3 Energy and efficiency calibrations

The film case of our spectrograph is equipped with notches which are used as geometric references. Indeed their locations to the source are known to 2/100 mm, which allowed us to establish the relation between the channel number in the spectrum and the distance on the film which is directly related to the curvature radius.

From the film obtained with the A = 187 sources, the $^{187}Au \rightarrow {}^{187}Pt$ electron lines corresponding to the exposure without preacceleration were used to determine the precise value of the magnetic field ($B = 54.43 \pm 0.03 \times 10^{-4}$ T) ; those corresponding to the exposure with preacceleration allowed us to define the value of the preacceleration high voltage with a 0.2 % accuracy. We have to note that in the space region where the magnetic and preacceleration electric fields are applied, the electron trajectories are no more circle arcs but elongated cycloids. However we have established that the trajectory from the

source to the film can be approximated to a circle arc provided that a linear dependence of the preacceleration high voltage upon the electron impact position on the film is introduced, which considerably simplifies the energy determination. We have checked that the error relative to this process was lower than 0.05 keV over the energy range whereas the total estimated error is 0.1 keV.

For intensity estimations, one of the most important parameters is the response of the detection system as a function of the electron energy. This response is difficult to obtain. Indeed it depends strongly on the nature of the photographic emulsion used and important fluctuations can be observed due to variations in the film processing. Moreover the dependence of the film response upon the electron intensity is linear only in a specific blackening-density range, beyond there is a film-saturation effect. To avoid this effect, we set a longitudinal shutter system inside the film case which allows us to obtain three different exposure times for each measurement. In this way, depending on its intensity, the electron line is analysed using one of these film

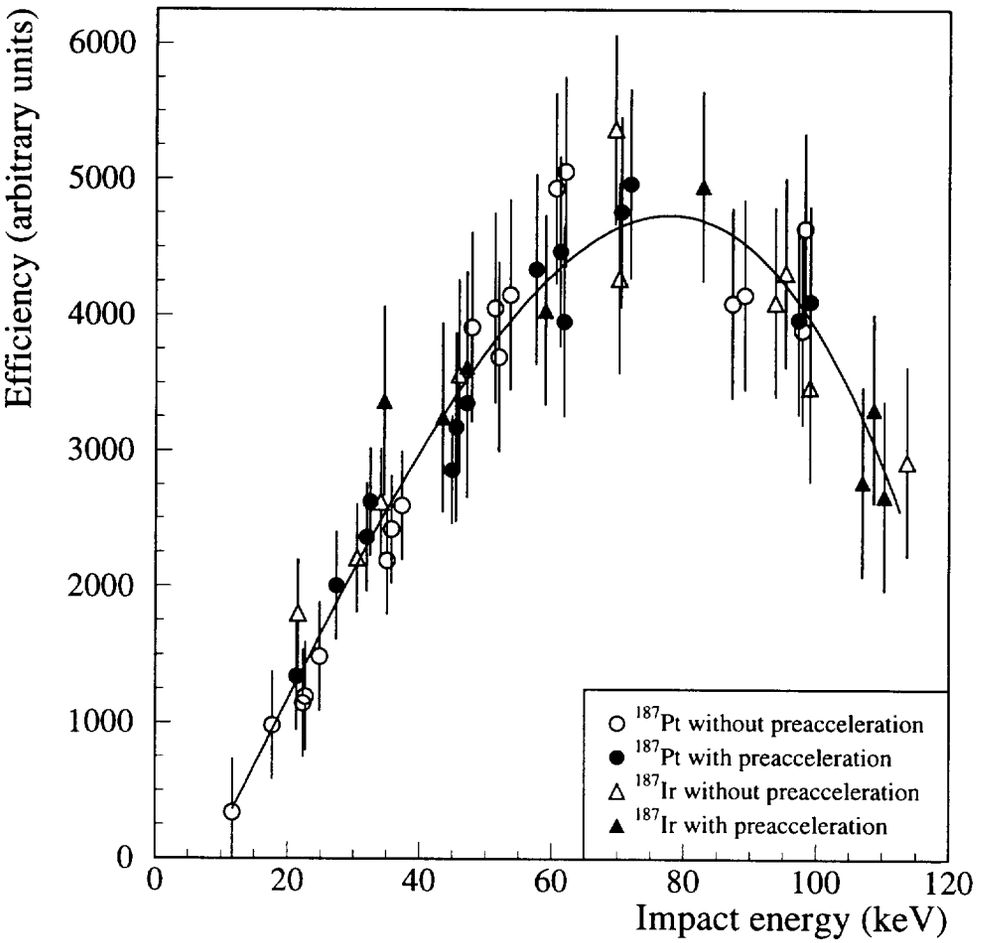

Fig. 1. Relative efficiency calibration of the spectrograph+film system measured as a function of the electron impact energy by using ^{187}Au and ^{187}Pt sources.

parts. Here, we restricted ourselves to determine globally the efficiency of the spectrograph+film system using the electron rays belonging to the ^{187}Au $\rightarrow$ ^{187}Pt decay, the intensities of which are well known in the 10 to 100 keV energy range [15]. Another efficiency determination has been made later using ^{187}Pt sources and the ^{187}Ir electron intensities extracted from ref. [16]. All the results are presented in fig. 1 where it is noticeable that the different data sets can be fitted by the same efficiency curve.

3 Experimental results

Figure 2 shows a partial electron spectrum obtained with ^{183}Hg sources. The high quality of the data is illustrated by the electron lines of the 16.0 keV transition in ^{183}Ir : the L_2 line, which corresponds to a 3.2 keV energy, is clearly observed and the doublet M_2-M_3, with a 0.36 keV energy difference, is well resolved. This is the first direct observation of the 16.0 keV transition in ^{183}Ir ; its multipolarity, obviously E2, confirms the interpretation proposed for the first excited level and the ground state linked by this 16.0 keV E2 transition [17]. This spectrum allowed us to determine the multipolarity of about twenty transitions in ^{183}Pt, ^{183}Ir, ^{179}Ir and ^{179}Os, the A = 179 mass chain being fed by the α-decay of ^{183}Hg.

In what follows, however, we will only display the results concerning the isomeric transition in ^{183}Pt. Electron lines arising from internal conversion in the L_1 and L_3 Pt electronic subshells have allowed us to pinpoint a 35.0 keV M3

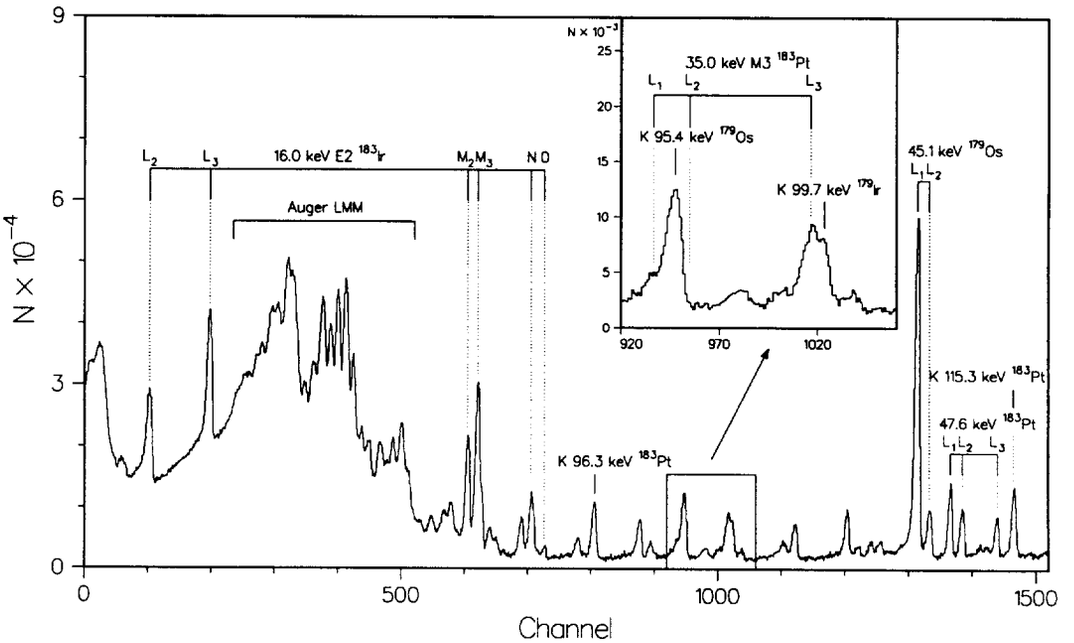

Fig. 2. Partial electron spectrum obtained with ^{183}Hg sources.

Table 1
Electron intensities, experimental L_3/L_1 and L_3/L_2 ratios for the 35.0 keV in ^{183}Pt and theoretical conversion coefficients [18] or ratios for various multipolarities.

	L_1	L_2	L_3	L_3/L_1	L_3/L_2
$I_{e^-}^{exp}$ a)	36 ± 7	< 36	179 ± 38	5.0 ± 1.4	> 5
M1	$1.87\ 10^1$	1.81	$2.00\ 10^{-1}$	0.0107	0.11
M2	$1.00\ 10^3$	$6.76\ 10^1$	$4.81\ 10^2$	0.481	7.11
M3	$2.16\ 10^4$	$1.51\ 10^3$	$1.04\ 10^5$	4.81	68.9
M4	$3.45\ 10^5$	$2.78\ 10^4$	$5.42\ 10^6$	15.7	195.0
E1	$3.69\ 10^{-1}$	$3.13\ 10^{-1}$	$4.04\ 10^{-1}$	1.09	1.29
E2	4.43	$2.42\ 10^2$	$2.68\ 10^2$	60.5	1.11
E3	$3.58\ 10^2$	$1.83\ 10^4$	$1.94\ 10^4$	54.2	1.06
E4	$9.41\ 10^3$	$5.66\ 10^5$	$6.07\ 10^5$	64.5	1.07

a) $I_{e^-}^{exp}$ obtained with $t_{collection} = t_{measurement} = 160$ s and normalized to the 115.3 keV ^{183}Au→^{183}Pt total intensity taken as reference (I_{tot}(115.3 keV) = 1000)

transition. One can see in the detailed part of fig. 2 that the L_3 electron line has been clearly observed and that the L_1 electron line has been detected, though it has a very weak intensity and it is mixed with another peak. The L_1 L_2 and L_3 intensities are compared in table 1 with the theoretical conversion coefficients for various multipolarities. This comparison supports with no doubt the M3 multipolarity for this 35.0 keV transition in platinum. The L_2 intensity is very difficult to extract because the L_2 line is mixed with the strong K line of the 95.4 keV transition in ^{179}Os. However one can estimate that it is weaker than the L_1 intensity, since no distortion is observed on the right side of the peak labelled K 95.4 keV in fig. 2. We conclude that the 35.0 keV transition is mainly M3 and contains less than 3 % E4.

The energy of the isomeric state in ^{183}Pt, indicated in ref. [6], is 34.3 keV. This value has been reevaluated to 34.50(8) keV by R.B. Firestone [19] using the data of ref. [6]. Thus, one can wonder whether the observed 35.0 keV M3 transition is actually the isomeric transition in ^{183}Pt. We have to note that, in the 0-160 keV range, the transition energies obtained for ^{183}Pt from the electron spectrum are systematically 0.2 or 0.3 keV higher than the values given in ref. [6], whereas the energy determination for the transitions belonging to the other nuclei present in the electron spectrum is in quite good agreement with what is known in the literature. This seems to indicate that the transition energies obtained in the present work are more accurate than those given in ref. [6]. Therefore we have determined the energy of the isomeric state taking

as energies for the transitions in the 0-160 keV range the values obtained from the electron lines observed in this work. In this way, the first two levels built on the ground state lie at 84.8 and 96.3 keV (instead of 84.6 and 96.0 keV in ref. [6]). These levels are both used to determine the energy of many other states and more especially the energy of the isomeric state which is found under these conditions to be 34.8 $\pm$ 0.2 keV. Moreover, we can note that, taking the energy of the isomeric state equal to 34.8 or 35.0 keV, the energy precision obtained for the levels, particularly for those located above 1.5 MeV, is in both cases better than 0.5 keV. Therefore we conclude that the 35.0 keV M3 transition observed in the electron spectrum is the isomeric transition in ^{183}Pt.

The percentage branching of the ^{183m}Pt decay by isomeric transition (b_{IT}) has been determined from the intensity of the M3 isomeric transition. Indeed the ratio between the ^{183m}Pt $\rightarrow$ ^{183g}Pt and ^{183}Au $\rightarrow$ $^{183m+g}$Pt disintegration numbers can be evaluated using : (i) the relative intensities obtained in the electron spectrum from the internal-conversion electron lines corresponding to the M3 transition and to other transitions in Pt and (ii) the ^{183}Au $\rightarrow$ ^{183}Pt level scheme. This ratio can also be expressed as a function of the timing conditions chosen to record the electron spectrum, the percentage branching of the ^{183m}Pt decay by isomeric transition and the half-lives of ^{183}Hg ($T_{\frac{1}{2}}$ = 8.8 s ref. [20]), ^{183}Au ($T_{\frac{1}{2}}$ = 42 s ref. [20]) and ^{183m}Pt ($T_{\frac{1}{2}}$ = 43 s ref. [21]). The experimental data lead to b_{IT} = 3.1 $\pm$ 0.8 %.

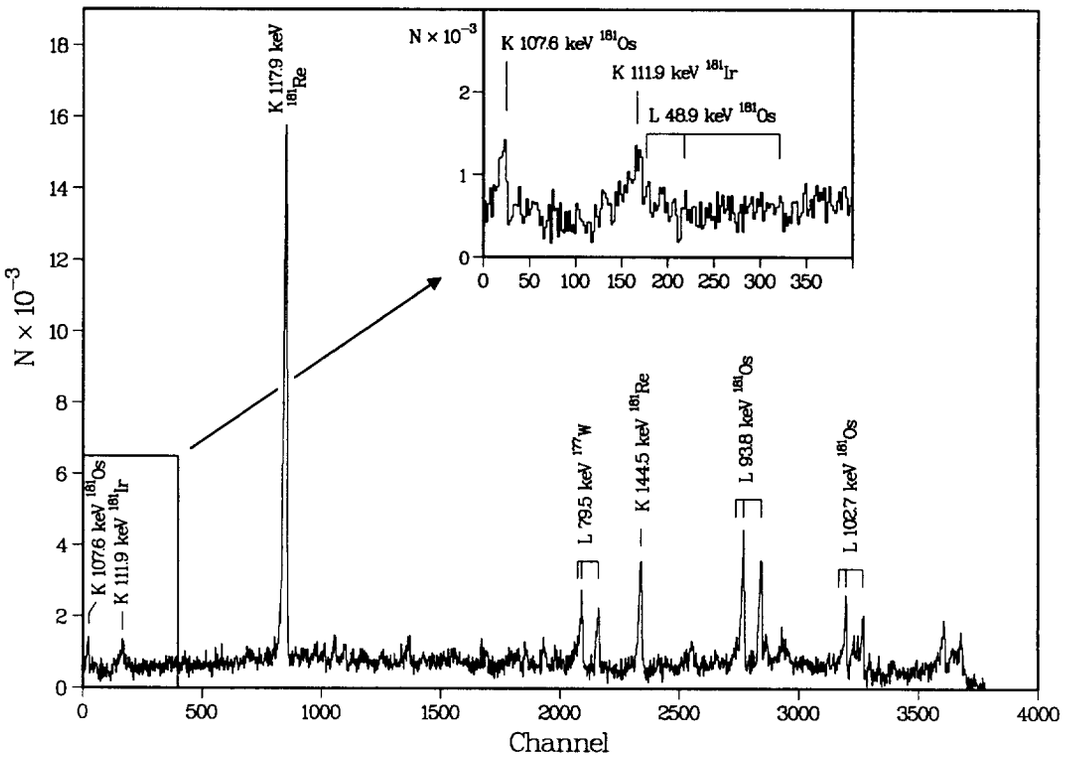

Fig. 3. Partial electron spectrum obtained with ^{181}Hg sources.

With regard to the search for the M3 transition in ^{181}Os, one can see in fig. 3 that no peaks appear in the spectrum at the positions expected for the L-electron lines corresponding to a 48.9 keV transition in Os, even though the energy of the transition would differ by 1.0 keV. In this case, only upper intensity limits can be estimated for the L_1, L_2 and L_3 electron lines. On the other hand, the K-electron lines of the 117.9 and 144.5 keV transitions belonging to the ^{181}Os $\rightarrow$ ^{181}Re decay appear strongly in the electron spectrum. Contrary to the 117.9 keV transition observed in both ^{181g}Os $\rightarrow$ ^{181}Re and ^{181m}Os $\rightarrow$ ^{181}Re decays, the 144.5 keV transition proceeds only from the ^{181m}Os $\rightarrow$ ^{181}Re decay and its multipolarity (E1) as well as its absolute intensity (I_γ = 87 %) are well established [22]. Therefore the comparison of the 144.5 keV line intensity extracted from the electron spectrum and of the upper intensity limit for the 48.9 keV L_3-ray (the strongest line expected for a multipolarity M3) leads to a direct estimate of the percentage branching of the ^{181m}Os decay by isomeric transition : $b_{IT} \leq 3$ %.

Table 2 presents the experimental M3 reduced transition probabilities calculated using the b_{IT} values obtained for ^{183m}Pt and ^{181m}Os. We have also reported the results related to the isomeric M3 transition in ^{179}W and ^{184}Au, both isotones of ^{183}Pt and ^{181}Os since the isomeric M3 transition consists in

Table 2
Experimental reduced M3 transition probabilities for the isomeric transition in ^{179}W, ^{181}Os, ^{183}Pt and ^{184}Au. In columns 5 and 6 are indicated the reduced M3 transition probabilities and Weisskopf hindrance factors for the $\nu\frac{1}{2}[521]\rightarrow\nu\frac{7}{2}[514]$ transitions.

Nucleus	E_γ (keV)	$I_i^\pi \rightarrow I_f^\pi$ ν configurations	$B^{exp}(M3)$ μ^2fm^4	$B(M3)$ μ^2fm^4	$F_W(M3)$ [a]
$^{179}_{74}$W [23]	221.9	$\frac{1}{2}^- \rightarrow \frac{7}{2}^-$ $\nu\frac{1}{2}[521]\rightarrow\nu\frac{7}{2}[514]$	0.92	0.92	1800
$^{181}_{76}$Os	48.9	$\frac{7}{2}^- \rightarrow \frac{1}{2}^-$ $\nu\frac{7}{2}[514]\rightarrow\nu\frac{1}{2}[521]$	$\leq$1.7	$\leq$6.8	$\geq$250
$^{183}_{78}$Pt	35.0	$\frac{7}{2}^- \rightarrow \frac{1}{2}^-$ $\nu\frac{7}{2}[514]\rightarrow\nu\frac{1}{2}[521]$	6.8 $\pm$ 1.8	27 $\pm$ 7	64^{+22}_{-14}
$^{184}_{79}$Au [2]	68.6	$2^+ \rightarrow 5^+$ $\nu\frac{1}{2}[521]\rightarrow\nu\frac{7}{2}[514]$ [b]	30 or 51	30 or 51	57 or 34

[a] $F_W(M3) = \frac{B_W(M3)}{B(M3,\ \nu\frac{1}{2}[521]\rightarrow\nu\frac{7}{2}[514])}$ with $B_W(M3) = 1.6501 \times A^{\frac{4}{3}}\ \mu^2fm^4$

[b] The π configuration is $\pi h\frac{9}{2}$ for both isomeric and ground states.

the $\nu\frac{1}{2}[521] \longleftrightarrow \nu\frac{7}{2}[514]$ one-particle transition for these four N = 105 isotones. Indeed, the neutron configurations $\nu\frac{7}{2}[514]$ and $\nu\frac{1}{2}[521]$ correspond respectively to the isomeric and ground states in ^{183}Pt and ^{181}Os and to the ground and isomeric states in ^{179}W. Concerning the ^{184}Au odd-odd nucleus, these two neutron configurations coupled to the same proton ($\pi h\frac{9}{2}$) have been proposed to describe the ground and isomeric states [4]. In order to compare the M3 reduced transition probabilities in these four N = 105 isotones, we have reported in columns 5 and 6 of table 2 the B(M3) values for the $\nu\frac{1}{2}[521] \rightarrow \nu\frac{7}{2}[514]$ transition and the Weisskopf hindrance factors.

4 Discussion

Before analysing the F_W(M3) values obtained in the N = 105 isotones, we shall recall some typical features on M3 transitions. Figure 4 shows the Weisskopf hindrance factors against the number of nucleons for all the known M3 tran-

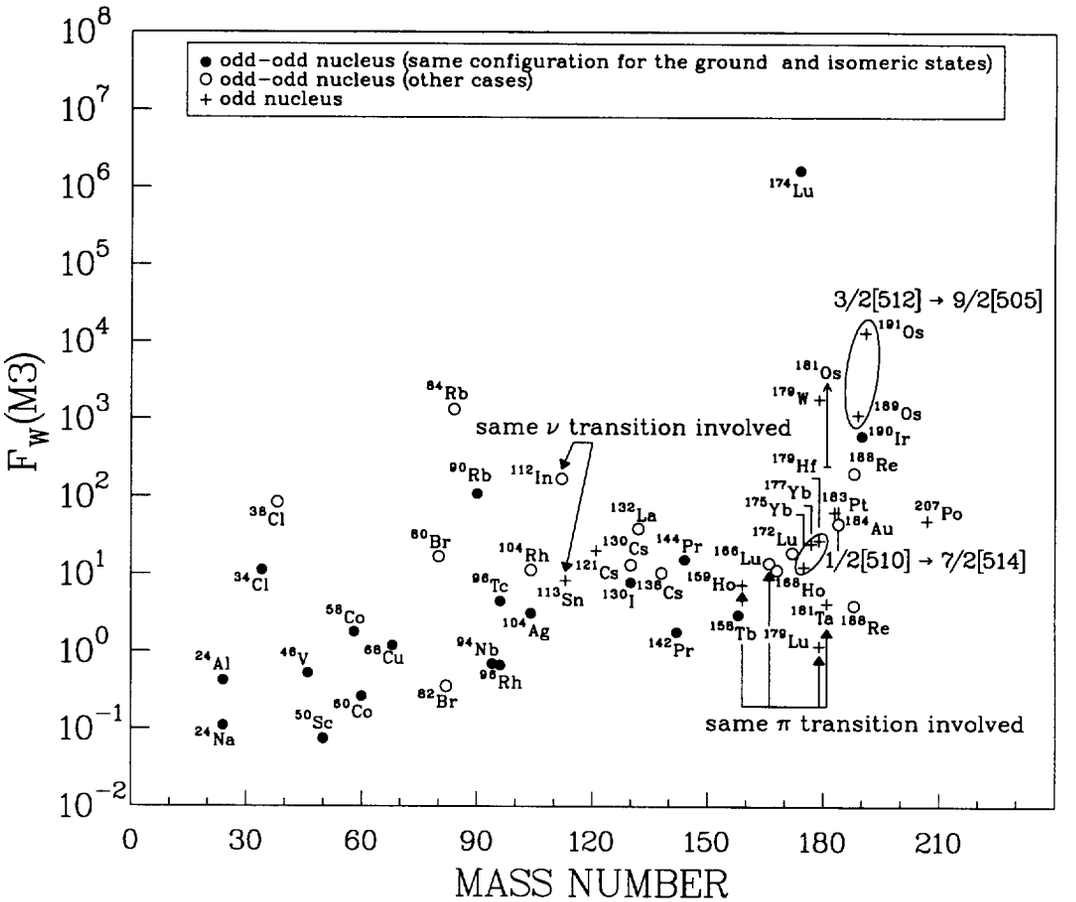

Fig. 4. Weisskopf hindrance factors for the known M3 transitions. Data are taken from ref. [24]. For ^{113}Sn, ^{181}Os, ^{183}Pt, ^{184}Au and ^{189}Os, the F_W values are those given in column 6 of tables 2 or 3.

sitions. The most striking characteristic is that the M3 transitions are very rare especially in odd-A nuclei : about fifty M3 transitions are known over the whole table of isotopes and among them, only fourteen in odd-A nuclei. Concerning these odd-A nuclei, it is worth noting that (i) most of the M3 transitions have been observed in heavy nuclei (A$\sim$180) and (ii) except for the Os isotopes, the F_W factors have similar values when the configurations describing the initial and final states are the same in several odd-A nuclei (see table 3). The $\nu\frac{3}{2}[512]\rightarrow\nu\frac{9}{2}[505]$ transition has to be considered as a special case since anomalies in the M3 conversion connected with a high γ-hindrance have been observed in ^{191}Os [25,26] but not in ^{189}Os. Concerning the odd-odd nuclei, the M3 transitions very often link states corresponding to the same $\pi \otimes \nu$ configurations but with Ω_p and Ω_n coupled antiparallel for one state and parallel for the other. In the other cases, and especially when the initial and final states differ only through the neutron or the proton configuration, which in the odd-odd nuclei implies a one-particle transition, the F_W factor is found higher in the odd-odd nucleus than in the odd-A neighbouring nuclei for the corresponding transition. Examples are given by the $\nu s_{\frac{1}{2}} \rightarrow \nu g_{\frac{7}{2}}$ neutron transition in ^{112}In and ^{113}Sn as well as the $\pi\frac{1}{2}[411]\rightarrow\pi\frac{7}{2}[404]$ proton transition in ^{166}Lu, ^{181}Ta, ^{179}Lu and ^{159}Ho (see table 3). Therefore, in spite of the scarcity of experimental data on M3 transitions, rules similar to those observed for transitions of lower multipolarity seem to arise and the analysis of B(M3) values appears to be an efficient means to investigate the structure of the initial and final states.

As regards the $\nu\frac{1}{2}[521]\rightarrow \nu\frac{7}{2}[514]$ M3 transition in the N = 105 isotones (see table 2), we note that the F_W(M3) values obtained in ^{183}Pt and ^{184}Au are similar, which tends to confirm the ν configurations attached to the isomeric and ground states in ^{184}Au. From the systematic comparison of F_W(M3) in odd and odd-odd nuclei, the M3 hindrance factor is expected to be lower in ^{183}Pt than in ^{184}Au, which is not actually the case. However, in ^{184}Au, one state having the same $\pi \otimes \nu$ configuration as the ground state is located at only 3.4 keV above the $I^\pi = 2^+$ isomeric state [4]. The presence of this state with $I^\pi = 2^+$ or 3^+ as possible spin and parity values could lead, in the case of $I^\pi = 2^+$, to a mixing in the wave function of the 2^+ isomeric state. Such an admixture could explain the finding of a F_W(M3) value smaller in ^{184}Au than in ^{183}Pt.

It appears also, from table 2, that the lower limit obtained for F_W(M3) in ^{181}Os is higher than the ^{183}Pt F_W(M3) value, but it is consistent with that in ^{179}W. Presently, we do not understand why such a dependence of F_W(M3) versus Z is observed in the N = 105 isotones for the $\nu\frac{1}{2}[521]\rightarrow \nu\frac{7}{2}[514]$ transition. Measurements with higher statistics would allow us to obtain a precise F_W(M3) value in ^{181}Os instead of a lower limit and to determine whether F_W(M3) varies progressively with Z or presents an abrupt change between ^{181}Os and ^{183}Pt. However, one can wonder whether the B(M3) evolution ob-

Table 3
M3 transition probabilities and Weisskopf hindrance factors for one-particle transitions in odd and odd-odd nuclei.

Nucleus	E_γ (keV)	$I_i^\pi \to I_f^\pi$ configurations	$B^{exp}(M3)$ μ^2fm^4	$B(M3)$ μ^2fm^4 configurations	$F_W(M3)$ [a]
^{191}Os	74.4	$\frac{3}{2}^- \to \frac{9}{2}^-$ $\nu\frac{3}{2}[512] \to \nu\frac{9}{2}[505]$	0.14	0.14 $\nu\frac{3}{2}[512] \to \nu\frac{9}{2}[505]$	13000
^{189}Os	30.8	$\frac{9}{2}^- \to \frac{3}{2}^-$ $\nu\frac{9}{2}[505] \to \nu\frac{3}{2}[512]$	0.63	1.6 $\nu\frac{3}{2}[512] \to \nu\frac{9}{2}[505]$	1120
^{179}Hf	160.7	$\frac{1}{2}^- \to \frac{7}{2}^-$ $\nu\frac{1}{2}[510] \to \nu\frac{7}{2}[514]$	62	62 $\nu\frac{1}{2}[510] \to \nu\frac{7}{2}[514]$	27
^{177}Yb	227.0	$\frac{1}{2}^- \to \frac{7}{2}^-$ $\nu\frac{1}{2}[510] \to \nu\frac{7}{2}[514]$	68	68 $\nu\frac{1}{2}[510] \to \nu\frac{7}{2}[514]$	24
^{175}Yb	514.8	$\frac{1}{2}^- \to \frac{7}{2}^-$ $\nu\frac{1}{2}[510] \to \nu\frac{7}{2}[514]$	129	129 $\nu\frac{1}{2}[510] \to \nu\frac{7}{2}[514]$	12.5
^{181}Ta	615.2	$\frac{1}{2}^+ \to \frac{7}{2}^+$ $\pi\frac{1}{2}[411] \to \pi\frac{7}{2}[404]$	405	405 $\pi\frac{1}{2}[411] \to \pi\frac{7}{2}[404]$	4.2
^{179}Lu	592.1	$\frac{1}{2}^+ \to \frac{7}{2}^+$ $\pi\frac{1}{2}[411] \to \pi\frac{7}{2}[404]$	1400	1400 $\pi\frac{1}{2}[411] \to \pi\frac{7}{2}[404]$	1.2
^{159}Ho	40.0	$\frac{1}{2}^+ \to \frac{7}{2}^+$ $\pi\frac{1}{2}[411] \to \pi\frac{7}{2}[404]$	193	193 $\pi\frac{1}{2}[411] \to \pi\frac{7}{2}[404]$	7.4
^{166}Lu	34.4	$3^- \to 6^-$ $\pi\frac{1}{2}[411] \to \pi\frac{7}{2}[404]$ [b]	108	108 $\pi\frac{1}{2}[411] \to \pi\frac{7}{2}[404]$	13.9
^{113}Sn	79.3	$\frac{7}{2}^+ \to \frac{1}{2}^+$ $\nu g\frac{7}{2} \to \nu s\frac{1}{2}$	27	108 $\nu s\frac{1}{2} \to \nu g\frac{7}{2}$	8.3
^{112}In	155.0	$4^+ \to 1^+$ $\nu s\frac{1}{2} \to \nu g\frac{7}{2}$ [c]	5.2	5.2 $\nu s\frac{1}{2} \to \nu g\frac{7}{2}$	171

[a] $F_W(M3) = \frac{B_W(M3)}{B(M3)}$ with $B_W(M3) = 1.6501 \times A^{\frac{4}{3}}\ \mu^2fm^4$

[b] the ν configuration is $\nu\frac{5}{2}[523]$ for both initial and final states

[c] the π configuration is $\pi(g\frac{9}{2})^{-1}$ for both initial and final states

Table 4
Nilsson M3 transition probability and hindrance factor for the $\nu\frac{1}{2}[521]\rightarrow\nu\frac{7}{2}[514]$ transition in ^{179}W, ^{181}Os and ^{183}Pt.

Nucleus	β_2 [a]	B_N(M3, $\nu\frac{1}{2}[521]\rightarrow\nu\frac{7}{2}[514]$)	F_N(M3) [b]
		μ^2fm^4	
$^{179}_{74}W_{105}$	0.26	431	468
$^{181}_{76}Os_{105}$	0.23	415	$\geq$61
$^{183}_{78}Pt_{105}$	0.20	374	14^{+5}_{-3}

[a] β_2 estimated from the energy of the first 2^+ level in the neighbouring even-even nuclei using the Grodzins empirical formula [28]

[b] $F_N(\mathrm{M3}) = \dfrac{B_N(\mathrm{M3},\ \nu\frac{1}{2}[521]\rightarrow\nu\frac{7}{2}[514])}{B(\mathrm{M3},\ \nu\frac{1}{2}[521]\rightarrow\nu\frac{7}{2}[514])}$ where B_N(M3, $\nu\frac{1}{2}[521]\rightarrow\nu\frac{7}{2}[514]$) is the Nilsson transition probability defined in ref. [27] and B(M3, $\nu\frac{1}{2}[521]\rightarrow\nu\frac{7}{2}[514]$) the value indicated in column 5 of table 2

served for the $\nu\frac{1}{2}[521]\rightarrow\nu\frac{7}{2}[514]$ transition through the N = 105 isotones can be explained by a change in deformation between the ^{179}W, ^{181}Os and ^{183}Pt nuclei. Transition probabilities as well as hindrance factors calculated in the frame of the Nilsson model [27] are presented in table 4. The B_N(M3) values appear to vary smoothly *vs.* β_2. The hindrance factor in ^{183}Pt is quite reasonable but the F_N(M3) value in ^{179}W is abnormally high whereas the selection rules for electromagnetic transition [29] indicate that the $\nu\frac{1}{2}[521]\rightarrow\nu\frac{7}{2}[514]$ transition with $\Delta\Omega = 3$, $\Delta N = 0$, $\Delta n_z = -1$ and $\Delta\Lambda = 3$ is not an M3 hindered transition.

5 Conclusion

Low-energy high-resolution internal-conversion-electron measurements have allowed us to determine the percentage branching of the ^{183m}Pt decay by isomeric transition. In the case of ^{181m}Os, only an upper limit of b_{IT} has been obtained. The reduced M3 transition probabilities have been calculated from the experimental results and compared to values known in the neighbouring odd (^{179}W) and odd-odd (^{184}Au) isotones. The B(M3) values are very similar in ^{183}Pt and ^{184}Au, which confirms the neutron configurations proposed to describe the isomeric and ground states in ^{184}Au. The limit obtained in ^{181}Os is consistent only with the ^{179}W value. The determination of a precise B(M3) value in ^{181}Os, instead of a limit, would allow us to check if there is a gradual variation versus Z or an abrupt change between ^{181}Os and ^{183}Pt. This sharp dependence of B(M3) against Z remains difficult to understand. The main

difference between the ^{179}W and ^{181}Os nuclei on the one hand, and the ^{183}Pt and ^{184}Au on the other hand, refers to nuclear deformation : the former are rather rigid and the latter exhibit indications of softness. Then the Nilsson model would be expected to describe the experimental results better in ^{179}W and ^{181}Os than in ^{183}Pt, which is not the case for the M3 transition probability between the $\nu\frac{1}{2}[521]$ and $\nu\frac{7}{2}[514]$ states discussed here. Abrupt changes in the hindrance factors of magnetic transitions between states having the same Nilsson orbital assignments are known since a long time. The case for M1 transitions in ^{181}Ta and ^{175}Lu has been carefully studied by S. Wahlborn and J. Blomqvist [30]. Their results brought interesting information concerning the effective M1 operator. In particular, they show that the tensor component is important to understand strong retardation of M1 transition. The N = 105 isotones with the $\nu\frac{1}{2}[521]\rightarrow\nu\frac{7}{2}[514]$ transition, as well as the Os isotopes with the $\nu\frac{3}{2}[512]\rightarrow\nu\frac{9}{2}[505]$ transition, may offer a possibility of similar studies in the case of M3 transitions. It constitutes a unique case of comparison of the effective magnetic operators of different multipolarity.

Acknowledgement

We would like to thank Dr N. Boos, R. Breuil, J.-F. Clavelin, M. Ducourtieux, A. Ferro, Dr D. Lunney, J. Munsch, J.-C. Potier and D. Sznajderman for technical support and help during the preparation and/or the running of the experiment. We are indebted to Dr C.F. Liang and G. Blain for the making of calibration sources. We also thank all the members of the ISOLDE group and specially J. Lettry for his work on the Pb target. Acknowledgements are due to S. Equilbey for his help with the microdensitometer operation. We are grateful to Dr R. Lombard for fruitful discussions and suggestions during the preparation of the paper.

References

[1] R. Eder, I. Berkes, D.E. Brown, I.S. Grant, E. Hagn, P. Harding, R. Hassani, P. Herzog, B. Kastelein, A. Knipper, G. Marguier, M. Massaq, S. Ohya, H. Postma, J. Prinz, C. Richard-Serre, I. Romanski, K. Schlösser, N.J. Stone, W. Vanderporten, J. Vanhaverbeke, L. Vanneste, T. Wölfle, E. Zech and the ISOLDE collaboration, *Proceedings of the 8th International Conference on Hyperfine Interactions, Hyp. Int.* **60** (1990) 83

[2] B. Roussière, J. Genevey, A. Gizon, F. Ibrahim, P. Kilcher, A. Knipper, F. Le Blanc, D. Lunney, G. Marguier, J. Oms, C. Richard-Serre, J. Sauvage and A. Wojtasiewicz, in: J. Kern, ed., *Proceedings of the 8th International Symposium*

on Capture Gamma-Ray Spectroscopy and related topics, (World Scientific, 1994) 231

[3] W.G. Nettles, R. Béraud, J.D. Cole, J.H. Hamilton, A.V. Ramayya, H. Kawakami, E.H. Spejewski and K.S.R. Sastry, *J. de Phys.* **39** (1978) 343

[4] F. Ibrahim, P. Kilcher, B. Roussière, J. Sauvage, J. Genevey, A. Gizon, A. Knipper, G. Marguier, D. Barnéoud, R. Béraud, G. Cata-Danil, J. Blachot, I. Deloncle, R. Duffait, A. Emsallem, D. Hojman, A.J. Kreiner, F. Le Blanc, J. Libert and J. Oms, *Z. Phys.* **A 350** (1994) 9

[5] F. Ibrahim, D. Hojman, A.J. Kreiner, B. Roussière, J. Sauvage, C. Bourgeois, A. Korichi, J. Davidson, M. Davidson, M. Debray, I. Deloncle, A. Knipper, F. Le Blanc, G. Marguier, J. Oms, N. Perrin, M.G. Porquet, H. Sergolle and H. Somacal, *Phys. Rev.* **C 53** (1996) 1547

[6] B. Roussière, C. Bourgeois, P. Kilcher, J. Sauvage, M.G. Porquet and the ISOCELE collaboration, *Nucl. Phys.* **A 504** (1989) 511

[7] B. Roussière, F. Ibrahim, P. Kilcher, F. Le Blanc, J. Oms, J. Sauvage, A. Wojtasiewicz and the ISOCELE collaboration, *Z. Phys.* **A 351** (1995) 127

[8] B. Harmatz, D.J. Horen and Y.A. Ellis, *Phys. Rev.* **C 12** (1975) 1083

[9] K.E.G. Löbner and S.G. Malmskog, *Nucl. Phys.* **80** (1966) 505

[10] W. Andrejtscheff, *Nucl. Phys.* **A 178** (1972) 563

[11] P.M. Endt, *Atom. Data and Nucl. Data Tables* **23** (1979) 3

[12] P.M. Endt, *Atom. Data and Nucl. Data Tables* **26** (1981) 47

[13] J. Lettry, R. Catherall, P. Drumm, A. Evensen, O. Jonsson, E. Kugler, J. Obert, J.C. Putaux, J. Sauvage, H. Ravn, M. Toulemonde and the ISOLDE collaboration, in: G.S. Bauer and R. Bercher, eds., *ICANS-XIII, Joint Proceedings of the 13th Meeting of the International Collaboration on Advanced Neutron Sources, PSI-Proc. 95-02* (Villigen, Switzerland, 1995) 595

[14] P. Kilcher, J. Sauvage, A. Wojtasiewicz, J. Munsch, J. Obert, A. Caruette, A. Ferro, G. Boissier, J. Fournet-Fayas, M. Ducourtieux, G. Landois, R. Sellem, D. Sznajderman and the ISOCELE collaboration, *Nucl. Instr. Meth.* **A 274** (1989) 485

[15] A. Ben Braham, V. Berg, C. Bourgeois, P. Kilcher, J. Letessier, M.G. Desthuilliers-Porquet, C. Schück, A. Huck, A. Knipper, C. Richard-Serre and A. Hoglund, *Nucl. Phys.* **A 332** (1979) 397

[16] C. Sébille-Schück, M. Finger, R. Foucher, J.P. Husson, J. Jastrzebski, V. Berg, S.G. Malmskog, G. Astner, B.R. Erdal, P. Patzelt, P. Siffert and the ISOLDE collaboration, *Nucl. Phys.* **A 212** (1973) 45

[17] C. Schück, A. Knipper, C. Richard-Serre, V. Berg, A. Zerrouki, J. Genevey-Rivier and the ISOLDE collaboration, in: J.H. Hamilton et al., eds., *Proceedings of the International Symposium on Future Directions in Studies of Nuclei far from Stability,* (North-Holland, Amsterdam, 1980) 127

[18] F. Rösel, H.M. Fries, K. Alder and H.C. Pauli, *Atom. Data and Nucl. Data Tables* **21** (1978) 92

[19] R.B. Firestone, *Nucl. Data Sheets* **65** (1992) 589

[20] P.G. Hansen, H.L. Nieken, K. Wilsky, M. Finger, A. Lindhal, R.A. Naumann and D.B. Nielsen, *Nucl. Phys.* **A 148** (1970) 249

[21] A. Visvanathan, E.F. Zganjar, J.L. Wood, R.W. Fink, L.L. Riedinger and F.E. Turner, *Phys. Rev.* **C 19** (1979) 282

[22] R.B. Firestone, *Nucl. Data Sheets* **62** (1991) 101

[23] E. Browne, *Nucl. Data Sheets* **55** (1988) 483

[24] *Table of Radioactive Isotopes,* (1986) V.S. Shirley, ed., for A = 24, 34, 38 ; *Nucl. Data Sheets* **56** (1989) for A = 84, 144 ; *Nucl. Data Sheets* **57** (1989) for A = 112 ; *Nucl. Data Sheets* **58** (1989) for A = 130 ; *Nucl. Data Sheets* **59** (1990) for A = 113, 188, 189 ; *Nucl. Data Sheets* **61** (1990) for A = 58, 190 ; *Nucl. Data Sheets* **62** (1991) for A = 174, 181 ; *Nucl. Data Sheets* **63** (1991) for A = 142 ; *Nucl. Data Sheets* **64** (1991) for A = 104, 121 ; *Nucl. Data Sheets* **65** (1992) for A = 132 ; *Nucl. Data Sheets* **66** (1992) for A = 80, 94 ; *Nucl. Data Sheets* **67** (1992) for A = 90, 166 ; *Nucl. Data Sheets* **68** (1993) for A = 46, 96, 177 ; *Nucl. Data Sheets* **69** (1993) for A = 60, 175 ; *Nucl. Data Sheets* **70** (1993) for A = 207 ; *Nucl. Data Sheets* **71** (1994) for A = 168 ; *Nucl. Data Sheets* **72** (1994) for A = 159, 179 ; *Nucl. Data Sheets* **74** (1995) for A = 138, 191 ; *Nucl. Data Sheets* **75** (1995) for A = 50, 172 ; *Nucl. Data Sheets* **76** (1995) for A = 68, 82 ; *Nucl. Data Sheets* **77** (1996) for A = 158 ;

[25] P. Loewenek and B. Martin, *Nucl. Phys.* **A 203** (1973) 332

[26] Yu. V. Sergeenkov and Yu. I. Kharitonov, *Izv. Akad. Nauk SSSR, Ser. Fiz.* **48** (1984) 926

[27] S.G. Nilsson, *Dan. Mat. Fys. Medd.* **29** (1955) 16

[28] L. Grodzins, *Phys. Rev.* **2** (1962) 88

[29] G. Alaga, *Nucl. Phys.* **4** (1957) 625

[30] S. Wahlborn and J. Blomqvist, *Nucl. Phys.* **A 133** (1969) 50